XXIV IMEKO World Congress "Think Metrology"
August 26 – 29, 2024, Hamburg, Germany

APPLICATION OF CALIBRATED X-RAY COMPUTED TOMOGRAPHY IN MICRO-SCALE HIDDEN STRUCTURE DIMENSIONAL MEASUREMENT

Shihua Wang

National Metrology Centre, Agency for Science, Technology and Research, Singapore
email address: wang_shihua@nmc.a-star.edu.sg

Abstract – In this paper, the XCT study investigates a high-density stainless steel dog bone sample, a low-density glass fiber with defects and standard artefacts including a hidden step height (nominal value: 120 µm, Type A1) and eight standard cylinders with certified reference diameters ranging from ϕ 0.1299 mm to ϕ 5.1960 mm. For the dog bone sample, its external dimensions up to 45 mm measured by XCT are compared favourably to corresponding dimensions measured by a calibrated digital caliper with a resolution of 0.01 mm. The deviation between XCT and the caliper is found to be less than 30 µm for millimetre dimensions up to 45 mm of the dog bone sample. The deviation of the hidden step height (nominal value: 120 µm) is less than 1.0 µm between XCT and a laser confocal microscope traceable to SI. The results indicate that XCT achieves accurate measurements for dimensions up to 45 mm and is effective in revealing hidden defects from 30 µm to 50 µm in the glass fiber sample. In addition, eight standard cylinders are measured by the proposed XCT, showing a maximum deviation from the reference diameter of less than 6.0 µm.

Keywords: Dimensional measurement; Measurement traceability; Hidden functional structure; Dog bone; Glass fiber; X-ray computed tomography (XCT)

1. INTRODUCTION

Advanced manufacturing including additive manufacturing (AM) process offers the capability to fabricate workpieces with intricate shapes and internal structures with applications in diverse industrial sectors such as Aerospace, Marine, Oil & Gas, and Medical. Ensuring the quality of fabrication involves non-destructively measuring micro-scale hidden structures in related parts, X-ray computed tomography (XCT) emerges as a promising tool for this purpose since it can penetrate hidden structures and provide dimensional information. However, there is lack of studies on measurement methodologies and verification data to establish dimensional measurement accuracy of XCT. This paper addresses this gap by applying XCT as a non-destructive, high-resolution tool to measure both external and internal geometrical features' dimensions.

The following non-destructive testing techniques [1-3], such as ultrasonic detecting sensor, thermal infrared imaging, shearography, and THz imaging, have been applied to locate internal defects and assess their dimensions. However, these techniques have limited identification resolution and typically provide either qualitative or only averaged dimensional information due to their working principles. In contrast, X-ray computed tomography (XCT) can conduct quantitative dimensional testing of samples by penetrating through different materials. The development of dimensional XCT covering micro and macro features [4,5] allows for the acquisition of both external and internal geometries at high sampling intervals along the testing parts in 3D.

As X-ray penetrates through the materials of the testing parts, the resulting XCT 3D images can provide detailed information about both external and internal dimensional structures. XCT enables the determination of external/internal dimensions and the location of hidden defects. Therefore, XCT is increasingly recognized as an internationally accepted testing tool by industry, offering geometric features' dimensional information in a wide range of applications for non-destructive quantitative measurement of both external and internal dimensions. X-ray computed tomography (XCT) is employed as a non-destructive high-resolution tool to measure both external and internal geometrical features' dimensions.

However, the contrast of dimensional XCT images heavily depends on the X-ray attenuation of the sample materials. Further studies are needed to assess the dimensional measurement quality and accuracy of XCT, especially for sample materials with high and low densities.

This paper utilizes several types of samples to showcase the dimensional measurement capabilities of XCT: a) A standard artifact, fabricated with a hidden step height (nominal value: 120 µm, Type A1) in accordance with ISO 5436-1, is employed to verify the micro-scale dimensional measurement accuracy of XCT. b) A high-density stainless-steel dog bone sample, with external dimensions in the tens of millimetres, is scanned by XCT to demonstrate its ability to properly penetrate dense materials and measure external dimensional lengths on a millimetre scale. c) A glass fiber, composed of fiber-reinforced plastic and composite material, is used to assess XCT's performance with materials of lower density but greater resistance compared to stainless steel.

Additionally, eight standard cylinders with certified reference diameters ranging from ϕ 0.1299 mm to ϕ 5.1960 mm are employed to evaluate XCT measurement non-linearity. Along with the related experimental results, it demonstrates XCT is a promising tool for conducting micro-scale external and internal dimensional measurements. The paper explores XCT's application in dimensional measurement using the high-density stainless-steel dog bone sample and a low-density glass fiber sample with defects.

2. DESCRIPTION OF SAMPLES

To simulate a hidden structure for checking XCT measurement accuracy, an assembled sample consists of a flat groove step (Nominal step: 120 µm; Width: 2 mm) on a substrate and a cover are fabricated. Noted that the step opening to air can be measured by a traceable laser confocal microscope for determining its actual step height. The assembled sample has a covered step to be measured by the proposed XCT. Therefore, step height deviation by XCT from the laser confocal microscope can be obtained to evaluate XCT results, which enables XCT measurement indirectly traceable to SI unit of metre definition.

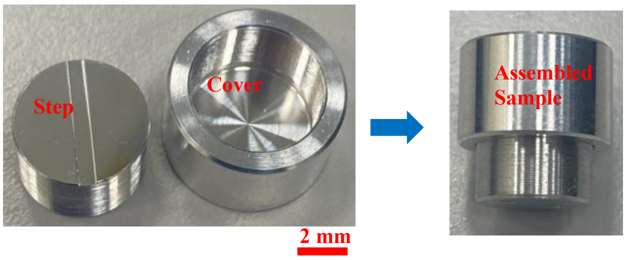

Figure 1. Photo of an assembled sample made from aluminium alloy.

Figure 2 shows a dog bone sample with different external dimensions. For a better future mechanical tension experiment of the dog bone sample, those dimensions need to be tested in advance. In this case, it is treated as a test coupon for evaluating XCT external dimensional measurement performance.

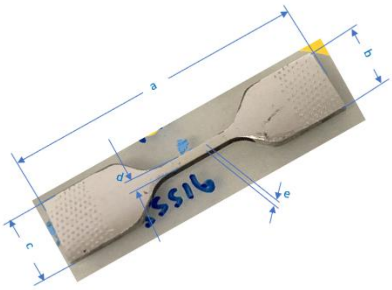

Figure 2. Photo of a dog bone sample with 5 external dimensions, nominally a = 45 mm, b & c = 10 mm, and d & e = 2 mm) to be measured to demonstrate XCT measurement capability of high dense hard stainless steel.

Figure 3 shows a glass fibre with 4 engineering defects inside glass fire. It can be seen that first two defects closer to label F1 is clearly observed, but last two are too blur to be observed. This is mainly because the last two is designed to have a thinner thickness than that of the first two. The objective is to identify the defect and measure its size using the proposed XCT.

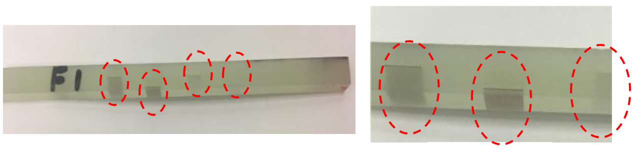

(a) (b)

Figure 3. Photos of (a) the glass fibre with its cross section by 5 mm ×5 mm and (b) Zoomed in photo to show the metal defect hidden in glass fibre.

3. METHODS

Figure 4 shows a setup diagram to indicate XCT utilized for the non-destructive testing of different materials. The XCT configuration includes X-ray source, a sample holder with rotary platform and an 2D array detector. Its X-ray energy is mainly adjusted by applied voltage and current onto X-ray source. The testing sample is mounted and fixed onto a precision rotating stage between the X-ray source and 2D array detector. The XCT system's geometrical configuration including magnification and volumetric pixel (voxel) size is calibrated by a certificated ruby ball bar. After X-ray going through the sample, an 2D X-ray image will have its contrast correlated to different X-ray paths through the sample. The resulting sample projected image onto the 2D array detector can be captured. A computer linked to the detector records a number of 2D X-ray attenuated image. Therefore, for forming an 3D XCT image, the rotating stage is then subsequently rotating till one circle of 360° rotation while corresponding X-ray image at each rotating position is accordingly recorded. Based on 2D XCT images obtained, an 3D XCT image can be reconstructed. The reconstructed 3D XCT image will be further processed using an XCT image process VG (Volume Graphic) [7], and the boundary from sample edge surface to the air can be determined to measure the interested dimensions.

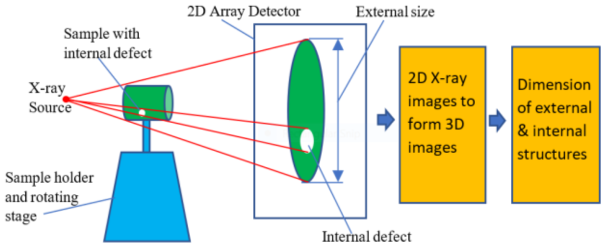

Figure 4. Schematic diagram of an XCT method.

4. Results and discussion

Figure 5 (a) and (b) show 3D and 2D XCT images of the assembled sample with a step groove scanned by the

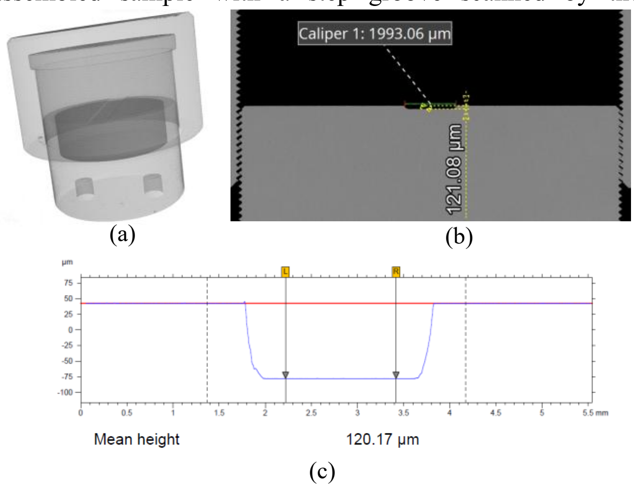

Figure 5. (a) An X-ray 3D image of the assembled sample with step. (b) Zoomed one cross- section of the Step image obtained by the proposed XCT. (c) One cross-section step profile obtained by a traceable laser confocal microscope.

proposed XCT with a voxel size at 10 µm. Its X-ray source attached with 0.1 mm Cu filter is powered at 120 KV and 100 µA. Figure 5(c) shows the measured result by a traceable laser confocal microscope (Resolution: 20 nm). It is found that the mean measured step height by XCT is 121.08 µm while a mean measured step height by laser confocal microscope is determined to be 120.17 µm with an expanded measurement uncertainty of 1.2 µm. The deviation of about 0.9 µm between XCT and laser confocal microscope is less than 1.0 µm or about 0.8% of the actual measured step height by the laser confocal microscope.

Figure 6 shows an XCT 3D image of the dog bone sample. In this case of the high dense stainless-steel dog bone sample , XCT voxel size is set to be 20 µm and X-ray source attached with 0.1 mm Cu filter is powered at 120 KV and 150 µA. Those 5 dimensions of the dog bone sample have been

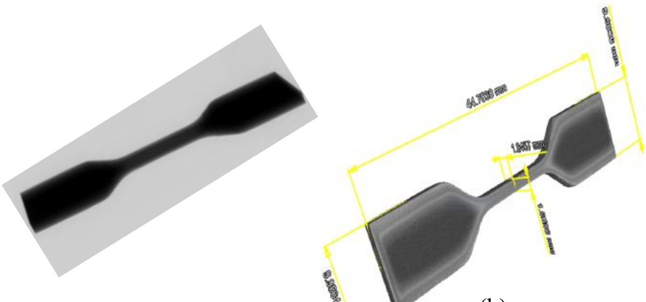

(a) (b)

Figure 6. (a) An X-ray image of the dog bone during XCT scanning. (b) Dog bone external dimensions are obtained by XCT.

determined by XCT. To verify XCT external dimensional measurement accuracy, the five dimensions are also measured by a digital caliper (resolution: 0.01 mm) uniformly along the dimensional features. Among those dimensions, it is observed that there is a slight measured deviation (-0.01 mm to 0.03 mm) between XCT and calibrated caliper as summarized in Table 1. This demonstrates that XCT

Table 1: Summary of five external dimensions (mm) measured by XCT and Calliper.

	No.	a	b	c	d	e
By Caliper (B)	1	44.74	9.97	9.99	1.65	1.84
	2	44.73	9.98	9.98	1.63	1.82
	3	44.74	9.95	9.96	1.62	1.83
	4	44.76	9.97	9.97	1.60	1.82
	5	44.76	9.96	9.99	1.64	1.84
	Average	**44.75**	**9.97**	**9.98**	**1.63**	**1.83**
	Standard Deviation	0.01	0.01	0.01	0.02	0.01
By XCT (A)		**44.78**	**9.96**	**9.98**	**1.63**	**1.85**
Difference (A-B)		0.03	0.01	0.00	0.00	0.02

dimensional measurement is favorably compared to the caliper measurement.

Figure 7 shows the result of glass fibre scanned by the proposed XCT. As can be seen, the glass fiber is clearly captured by XCT. To have a larger field view in XCT, the XCT is set (Magnification: 4×; Voxel Size: 25 µm) to cover 4 defects inside the glass fiber.

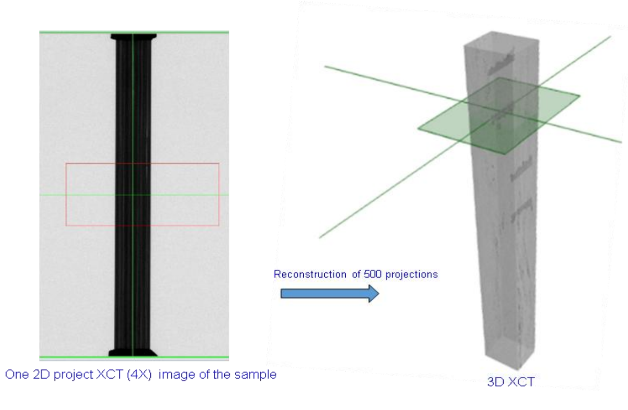

(a) (b)

Figure 7. (a) A 2D projection image of the glass fibre bar. (b) 3D XCT image obtained.

In Figure 8, it is seen that two defects next to label F1 at the top position of the glass fibre have clearly been identified.

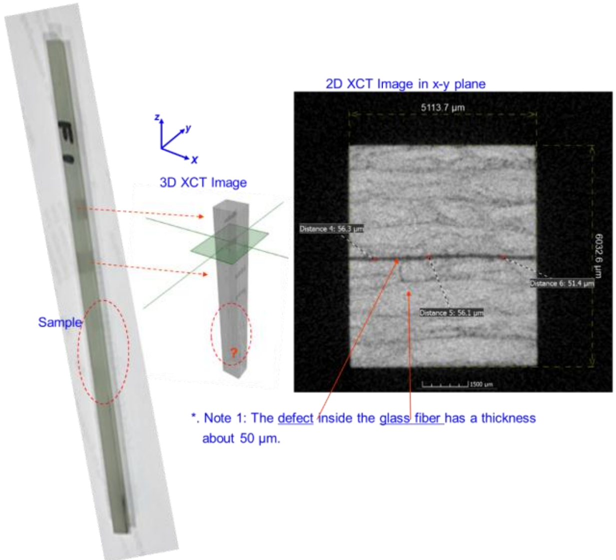

Figure 8. 2D XCT image to show a defect identified as in x-y plane perpendicular to the defect square.

Their locations are highlighted by two dashed line arrows. In 2D XCT image of x-y plane across the defect, the dark gap within the glass fiber is the defect to be measured in a thickness of 50 µm.

Figure 9 shows that the defect was measured in a size of 5044.7 µm ×5317.5 µm and it is found that the square defect

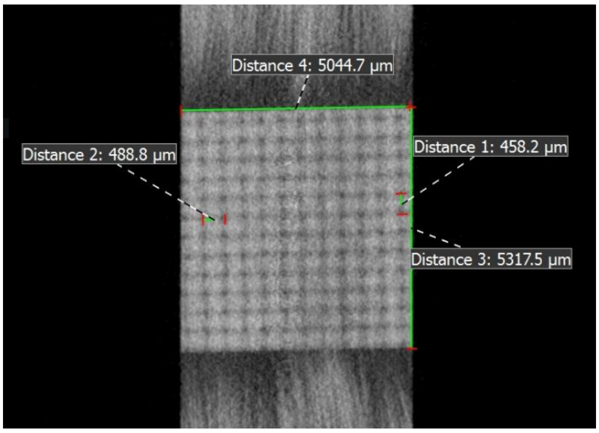

Figure 9. 2D XCT image to show a defect identified as in y-z plane parallel to the square defect.

has 458.2 µm × 488.8 µm gird holes within the defect area. However, due to a lower XCT magnification (4×, Voxel size: 25 µm), another two defects highlighted by a dashed elliptic circle in Figure 8 are still not resolved in XCT image since those two defects have thinner thickness. After enlarging XCT magnification (20×, Voxel: 5 µm), the area with two thinner defects is re-scanned by XCT as shown in Figure 10.

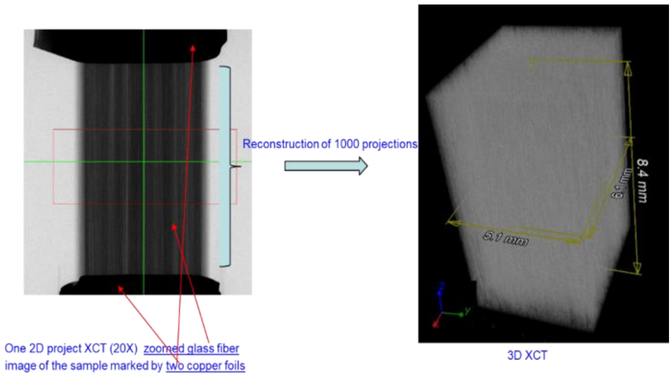

Figure 10. 2D XCT image to show a zoomed in area having the thinner defect and 3D XCT already indicate the bundle of fibres are laminated in a square bar shape.

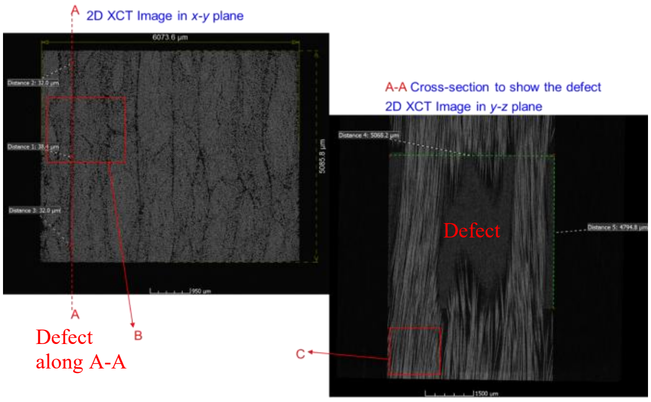

(a) (b)

Figure 11. (a) An enlarged 2D XCT images to show more details of individual fibre and the defect. The defect thickness is ranging from 32.0 µm to 38.4 µm. (b) The identified defect along A-A cross-section in Figure 11(a) is shown in Figure 11(b).

As shown in Figure 11, it is seen that details of the fibres and defect are disclosed in 2D XCT images. Based on 2D XCT images in Figure 11, two zoomed images from areas B and C

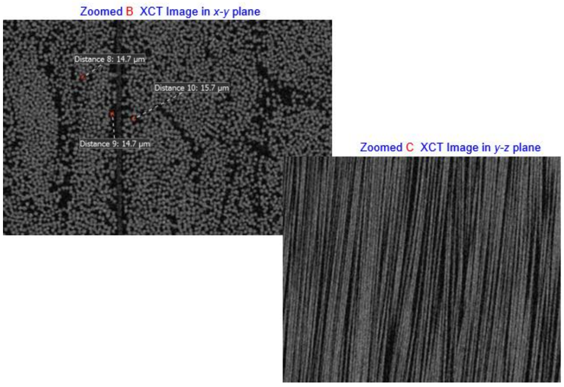

Figure 12. Zoomed in 2D XCT images to show the defect and individual fibres are all clearly observed.

are enlarged in Figure 12. It is seen that the thinner defect's thickness is not uniform. The individual fibre diameter is measured to be 14.7 µm and 15.7 µm, respectively. In addition, it is found that there are some voids among those fibres inside the glass fibre bar. This indicates glass fibre lamination uniformity quality needs to be improved as well.

To verify XCT's linear measurement accuracy, a set of standard cylinders with certified diameters is measured respectively by XCT. Their reference diameters are shown in Table 2.

Table 2. List of standard cylinders used to verify XCT's linear measurement accuracy.

Sample, No.	Ref Diameter (µm)
1	129.9
2	346.6
3	866.2
4	1154.7
5	2020.9
6	2886.8
7	4041.7
8	5196.0

Figure 13 shows 3D XCT images of 2 standard cylinders.

Figure 13. Examples to show XCT images of 2 standard cylinders measured diameters of ϕ 132.3 µm and ϕ5199.8 µm by the proposed XCT.

Figure 14 shows those measured diameters versus reference values. The maximum deviation is found to be 5.9

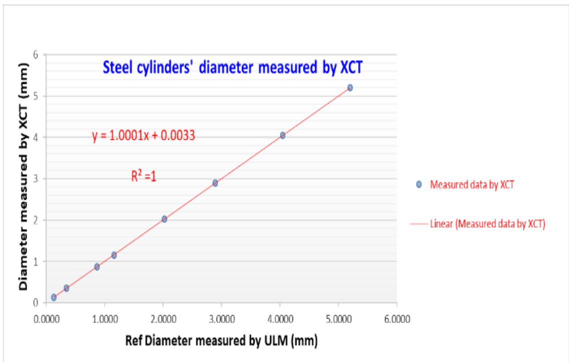

(a)

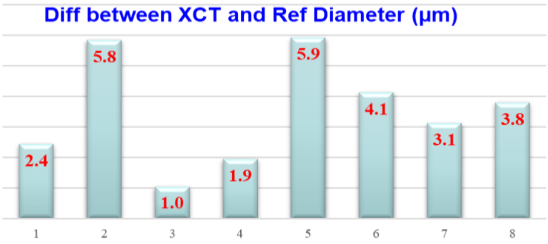

(b)

Figure 14. (a) Plot to show XCT dimensional measuring non-linearity. and (b) Deviation between XCT results and reference values.

µm. By considering the diameter range from 129.9 µm up to 5196.0 µm, a measurement non-linearity is found to be 0.11% (5.9 µm/5196.0 µm) for XCT to measure diameter. Therefore, the measurement error of defect from 30 µm to 50 µm and fibre diameter about ϕ 15 µm can be estimated.

5. CONCLUSIONS

The samples, including a stainless-steel dog bone and a glass fiber with defects, were successfully measured using the proposed X-ray computed tomography (XCT) with optimized parameters to enhance image quality and achieve higher measurement resolution. Experimental results demonstrate that higher magnification leads to better XCT resolution, allowing for clear identification of detailed structures such as defects hidden inside laminated glass fibers.

Quantitatively, the internally hidden step height (nominal value: 120 µm) measured by the proposed XCT shows less than 1% deviation from values obtained by a traceable laser confocal microscope. External dimensions (typically 45 mm, 10 mm, and 2 mm) measured by the proposed XCT exhibit deviations of less than 0.03 mm compared to calibrated digital caliper (resolution: 0.01 mm). Additionally, the thickness and diameter of fibers hidden inside laminated glass fibers are determined to be approximately 30 µm to 50 µm and ϕ15 µm, respectively.

In summary, the promising measurement results suggest that the proposed XCT method for measuring external and internal dimensional structures can serve as a benchmark tool, providing reference standards for external dimensions and internal hidden defects used to characterize the performance of other non-destructive testing tools. Furthermore, it has the potential to be further developed for calibration and measurement of complex structures inaccessible by conventional metrology equipment.

ACKNOWLEDGMENTS

This work was financially supported by A*STAR, RIE2025 Manufacturing, Trade and Connectivity (MTC) Fund: Advanced models for Additive Manufacturing (AM2) [Grant No.: M22L2b0111].

REFERENCES

[1] Philip J. Withers, Charles Bouman, Simone Carmignato, Veerle Cnudde, David Grimaldi, Charlotte K. Hagen, Eric Maire, Marena Manley, Anton Du Plessis & Stuart R. Stock, X-ray computed tomography, Nature Reviews Methods Primers volume 1, Article number: 18 (2021)

[2] K.S.Vaghosi, G.D.Acharya, Review on Defects in GFRP Composites, International Journal of Advance Engineering and Research Development , Volume 4, Issue 9, September -2017.

[3] Kumar Anubhav Tiwari, ID and Renaldas Raisutis, Identification and Characterization of Defects in Glass Fiber Reinforced Plastic by Refining the Guided Lamb Waves, Materials 2018, 11, 1173.

[4] J. P. Kruth, M. Bartscher, S. Carmignato, R. Schmitt, L. De Chiffre, A. Weckenmann, 'Computed tomography for dimensional metrology', CIRP Annals – Manufacturing Technology 60, pp821-842, 2011

[5] Anton du Plessis, Igor Yadroitsev, Ina Yadroitsava and Stephan G. Le Roux, X-Ray Microcomputed Tomography in Additive Manufacturing: A Review of the Current Technology and Applications, 3D PRINTING AND ADDITIVE MANUFACTURING, Volume 5, Number 3, pp227-247, 2018

[6] P. K. Mallick, Fiber-Reinforced Composites: materials, manufacturing, and design, 2007.

[7] VG website available September 2023: https://www.volumegraphics.com/